This document is currently under revision by the European Commission (EC) and has not yet been validated or approved by the EC. The content provided herein is subject to change, and the information presented may not represent the final position or official stance of the EC.

This document is being shared for informational purposes only and is not to be considered an official or authoritative source of information from the European Commission. Any decisions, actions, or interpretations based on the content of this document should be taken with caution, as the content may be subject to modification or revision by the EC.

The EC accepts no liability for any inaccuracies, errors, or omissions in this document, and any reliance on its content is at the user's own risk. It is recommended to verify the information provided in this document with official EC publications or communications before making any decisions or drawing any conclusions based on its content.

Please note that the content in this document may be confidential or sensitive in nature and should be treated as such. Unauthorized dissemination, distribution, or use of this document is strictly prohibited.

By accessing and reviewing this document, you acknowledge and accept the terms of this disclaimer.

BL2F

Transforming Black Liquor to Biofuel

Research and Innovation Action
H2020-LC-SC3-2019-NZE-RES-CC

D1.6 - Process scale-up modelling tool and CFD modelling reports

WP1 - Task 1.6

December 2023 [M45]

Lead Beneficiary: Tampere University

Author(s): Huila Joona (TAU), Vaibhav Agrawal (TAU), and Joronen Tero (TAU)

@BL2F_EU

www.bl2f.eu

BL2F_EU

Disclaimer

The content of this deliverable reflects only the author's view. The European Commission is not responsible for any use that may be made of the information it contains.

This project has received funding from the European Union's Horizon 2020 research and innovation programme under the Grant Agreement n°884111.

Document Information

Grant agreement	884111
Project title	Black Liquor to Fuel by Efficient Hydrothermal Application integrated to Pulp Mill
Project acronym	BL2F
Project coordinator	Prof. Dr. Tero Joronen
Project duration	1st April 2020 – 31st March 2024 (48 Months)
Related work package	WP 1 - HTL-oil production
Related task(s)	Task 1.6 - Scale-up model for IHTL process
Lead organisation	TAU
Contributing partner(s)	TAU
Due date	31st December 2023
Submission date	20th December 2023
Dissemination level	Public

History

Date	Version	Submitted by	Reviewed by	Comments
15th Dec. 2023	N°1	Huila, Agrawal, and Joronen	Konttinen and Arjmand	

Table of contents

List of figures

List of tables

Abbreviations and acronyms

Acronym	Description
BL	Black Liquor
CFD	Computational Fluid Dynamics
EHTA	Equipment for Hydrothermal Applications (Pilot at TAU)
GC-MS	Chromatography-Mass Spectrometry
HHV	Higher Heating Value
HTL	Hydrothermal Liquefaction
IHTL	Integrated HTL (combination of HTL and salt separation)
LHV	Lower Heating Value
SST	Shear Stress Transport (turbulence model)
TAU	Tampere University
TRL	Technology Readiness Level (0 – 9, idea to fully commercial)

Executive Summary

The BL2F project (#884111) studies conversion of Black Liquor to Sustainable Aviation and Marine biofuels. A process scale-up tool with Aspen Plus was developed. Computational Fluid Dynamics (CFD) was applied to study the novel design of the combined HTL and salt separator reactor.

The scale-up model can predict rather realistic behaviour of the process in the yield, gas generation, pressure dependence, and dilution of the feed. The scale-up model can be utilized in studying and designing of the demonstration plant in the next development step of the technology.

The CFD model was used in the case study of the novel IHTL reactor construction to have insight of the flow and temperature patterns inside the reactor. The desired two reaction zones, top part in super-critical conditions for fast HTL reactions, and lower part for the collection of the brine were applied to being maintained in different conditions. Also, the feed was well and evenly mixed into the reaction zone. The experience from the test runs supports the findings, as we have not experienced any blocking or contamination inside the reactor. The CFD model can be applied to study the scaling up of the reactor in the next step.

Keywords

Advanced HTL, Black liquor, Fuel, Aviation, Shipping, Scale-up, Process Model, CFD model, Reactor design

1 Introduction

The European project Black Liquor to Fuel (BL2F, #844111) aims to develop an advanced HTL conversion technology that utilizes the side-stream of Kraft Pulping Black Liquor (BL) to Aviation and Marine fuels. The BL is mainly consisting of the remaining of the wood after extraction of pulp in the digestions, and the cooking chemicals (mostly Sodium Carbonate). The benefit of the BL as a feed to HTL are homogenous quality and pumpability as a fluid. The integration of HTL technology to a Pulp Mill has several benefits mainly being existing equipment for the handling of the returning flows and heat and operational integrations.

In the BL2F project the technology is tested and moved to the TRL level of 5. To be able to scale up the technology models are developed utilizing process and computational fluid dynamics (CFD) software. This report introduces the process scale-up tool build with Aspen Plus and the CFD modelling of the IHTL reactor. First the Process scale-up tool is presented in part 2. The part 3 presents the CFD studies. Both parts end to conclusions.

2 Process scale-up modelling tool

2.1 Materials and methods

2.1.1 Model overview

The model flowsheet was developed based on Lappalainen's model (2018), incorporating elements from existing hydrothermal liquefaction models. Black liquor and water are introduced into the reactor through separate lines (Figure 1). Both feedstock lines are pressurized to the desired level (300 bar) using designated pumps. Following pressurization, the temperature is elevated into the supercritical region (above 374 °C). Each line integrates a heat recovery system, with black liquor heated by recuperating heat from the hot product post-hydrodeoxygenation. The flushing water line is linked to the hot brine line. External heaters are employed for further heating or temperature adjustment in both black liquor and flushing water lines.

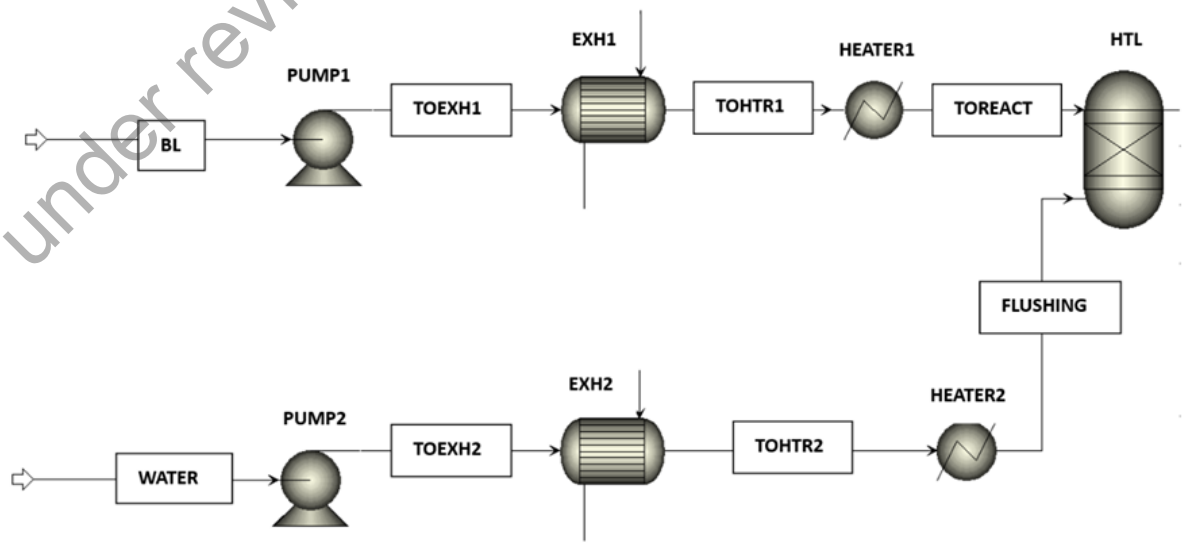

Figure 1: Feeding Lines for Black Liquor and Water, Including Pressurizing and Heating

Within the reactor, black liquor and flushing water are combined, and hydrothermal liquefaction reactions take place. In the pilot reactor, geometry and flushing positioning influence the process. The feeding rate can be modulated by adjusting the flow rate of flushing water. The model assumes perfect mixing inside the reactor. Gibbs free energy minimization is employed to estimate the fractions of produced components in hydrothermal liquefaction reactions. The method relies on equations from calculation theory, automatically calculated by Aspen Plus. The selection of this method is influenced by previous studies and considerations regarding the inaccuracies associated with kinetic modelling, as highlighted by Lappalainen in his simulation model. However, the equilibrium model allows for a more convenient sensitivity analysis. For enhanced accuracy, reactions and residence times should be considered since reaching total equilibrium in the process is unlikely. The Soave-Redlich-Kwong (SRK) equation of state is chosen as a property method due to its suitability for equilibrium-based modelling in high-temperature and pressure ranges.

After the hydrothermal liquefaction (HTL) reactor, inorganic compounds are separated in the form brine from HTL products. In the continuous pilot reactor, ideal solid separation occurs concurrently with HTL reaction, and brine is collected from the reactor's bottom. In this simulation model, solid separation is depicted as an individual step (Figure 2). The brine contains inorganic salts and organic hydrochar. Additionally, some water is removed along with the brine, referred to as wastewater and separated from solid material later.

Biocrude is enriched through an integrated hydrodeoxygenation process where external hydrogen is introduced to decrease the oxygen content in biocrude. Although an equilibrium-based reactor type is utilized, it may not be the most realistic solution. Nevertheless, an increase in the H/C ratio is observed, allowing for a rough estimation of the hydrodeoxygenation effect. The method for hydrogen production is not detailed here but is crucial for evaluating the process's cost and environmental impacts.

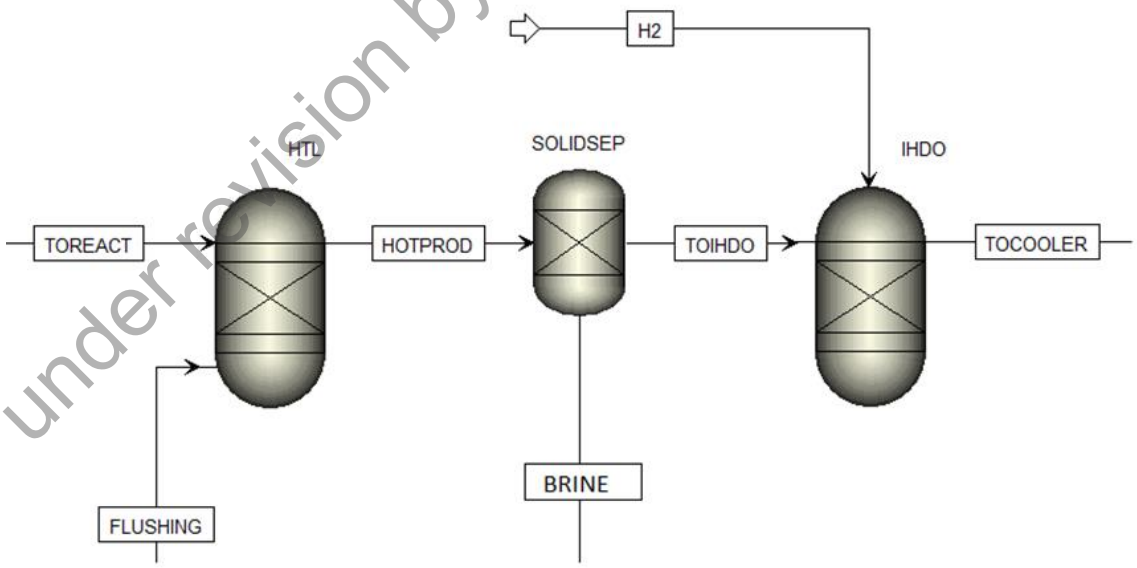

Figure 2: Reactor Followed by Solid Separation and Integrated Hydrodeoxygenation Process

The heat energy from hot brine and hot product is recovered, as mentioned earlier. External coolers are incorporated into both brine and product lines for additional cooling if needed. Pressure reduction is achieved through depressurizing pumps after cooling. The aqueous phase and gases are separated from biocrude (Figure 3). This step is included in the model to approximate biocrude yield and component fractions. In real-world scenarios, phase separation is more complex, requiring consideration and further study of efficient separation methods.

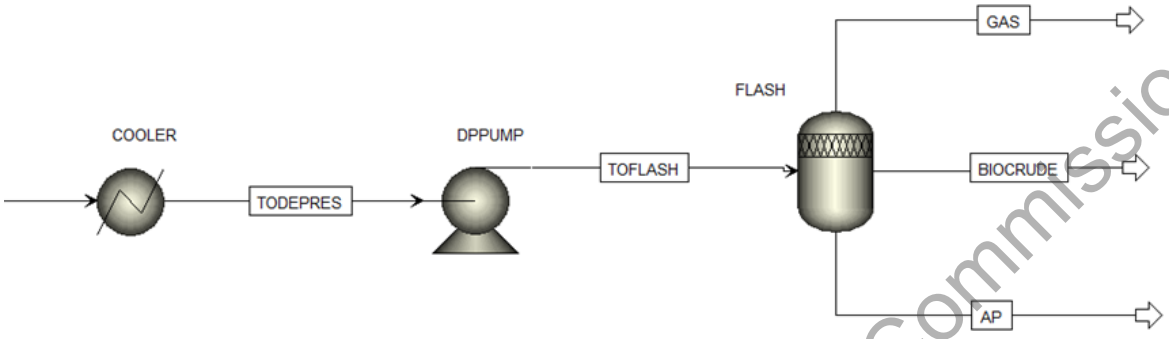

Figure 3: Phase Separation of Biocrude, Gas, and Aqueous Phase

The scale-up from pilot reactor size was primarily achieved by increasing the volumetric flow of black liquor and flushing water. Adjustments to the parameters of heat exchangers were necessary due to increased flows. In this case, the volumetric flow of black liquor was scaled-up to 1 kg/s, close to the targeted industrial scale. However, some fine-tuning may be necessary to account for variations in sizes among different industrial plants in different locations. The whole process flow chart including heat integration is shown in appendix A.

2.1.2 Model compounds

The composition of dry black liquor employed in this model is delineated in Table 1, with characterization informed by the research conducted by Magdeldin et al. (2020). The black liquor composition emulates that of Kraft softwood-derived black liquor, drawing from pertinent literature and stakeholder discussions. Notably, the water content of black liquor in this study is specified as 82 wt.%. Lignin is initially modelled as a non-conventional compound at the onset of the process but is subsequently transformed into coniferyl alcohol ($C_{10}H_{12}O_3$), aligning with the modelling approach introduced by Lappalainen.

Table 1: Model compounds used in black liquor modelling (Magdeldin et al. 2020)

Species	Model compounds	Molecular formula	Wt.% (dry)
Polysaccharides (2 %)	Glucose/Dextrose	$C_6H_{12}O_6$	2.00
Aliphatic salts (40 %)	Sodium acetate	CH_3COONa	40.00
Extractives (4 %)	Oleic Acid	$C_{18}H_{34}O_2$	3.05
	AbieticAcid	$C_{20}H_{30}O_2$	0.95
Kraft Lignin (28 %)	Non-conventional compound	$C_{9.6}H_{9.6}O_{3.1}S_{0.65}N_{0.006}$	28.00
Lignin Derivatives (3 %)	Phenol	C_6H_6O	0.03
	2-Methylphenol	C_7H_8O	0.02
	4-Methylphenol	C_7H_8O	0.04
	Guaiacol	$C_7H_8O_2$	0.61
	Creosol	$C_8H_{10}O_2$	1.34
	Eugenol	$C_{10}H_{12}O_2$	0.56
	Vanillin	$C_8H_8O_3$	0.22
	Acetoguaiacone	$C_9H_{10}O_3$	0.16
	Syringol	$C_8H_{10}O_3$	0.02
	Syringaldehyde	$C_9H_{10}O_4$	0.01
Miscellaneous (1 %)	Catechol	$C_6H_6O_2$	0.06
	Thiophene	C_4H_4S	0.06
	Cyclopentane	C_5H_{10}	0.06
	Methanol	CH_3OH	0.50
	Alpha-Pinene	$C_{10}H_{16}$	0.11
	Methyl Mercaptane	CH_4S	0.11
	Dimethyl sulfide	C_2H_6S	0.11
Inorganics (22 %)	Sodium hydroxide	NaOH	1.32
	Sodium sulfide	Na_2S	3.74
	Sodium carbonate	Na_2CO_3	7.04
	Potassium hydroxide	KOH	0.88
	Potassium carbonate	K_2CO_3	0.88
	Potassium chloride	KCl	0.44
	Sodium chloride	NaCl	0.44
	Sodium sulfate	Na_2SO_4	7.26

The selection of model compounds for biocrude is intricate, as it hinges on both the process parameters of hydrothermal liquefaction and the composition of black liquor. The number of

real compounds in biocrude can range from hundreds to thousands, with aromatic compounds being the desired products in the hydrothermal liquefaction of lignin (Woerner et al. 2022). Two distinct cases for selected model compounds for biocrude are explored in this work to discern the impact of different compounds within an equilibrium model. The model compounds for both cases are enumerated in Table 2.

Table 2: Model compounds selected for biocrude modelling

Case 1	Case 2
Phenol	Phenol
Palmitic acid	Anisole
	p-Cresol
	Guaiacol
	2-2'-Methylenediphenol
	o-Acetylphenol
	1,2-dimethoxybenzene
	9H-xanthene
	2-Benzyl-4-methoxyphenol
	Retene
	Undecadiynoic Acid

In the first case, model compounds for biocrude are limited to two compounds: palmitic acid ($C_{16}H_{32}O_2$) and phenol (C_6H_6O), reflecting their high abundance in the GC-MS analysis of biocrude resulting from the hydrothermal liquefaction of diverse biomass feedstocks. The cyclic structure of phenol provides insights into the behaviour of many other compounds found in biocrude (Qian et al. 2021). This selection aims to maintain model simplicity without compromising reliability. In the second case, a more realistic and diverse range of model compounds is employed, based on a study by Ong et al. (2018), where the composition of biocrude was identified by GC-MS analysis and approximated by selecting the dominant component of each functional group. The model is initially constructed using the model compounds from case 1 and further refined based on results derived from sensitivity analysis.

2.2 Results and discussion

The simulation model underwent testing at a temperature of 375 °C and a pressure of 300 bar, selected based on precedent studies and congruent conditions at the pilot facility. The chemical equilibrium in the reactor was determined by the interplay of salts and chosen model

compounds. Char formation, deemed relatively low, was included in solid phase. Inorganic compounds were designated as brine and separated before subjecting the product to hydrodeoxygenation. Total mass yields, calculated based on the dry content of black liquor, are presented in Table 3.

Table 3: Yields of Hydrothermal Liquefaction Products at 375 °C and 300 bar

	Yields (m-%)
Biocrude	48.0
Solid (Salts + char)	44.5
Gas	7.7

All organic model compounds were converted into biocrude and gases. Biocrude comprised both palmitic acid and phenol, while the gaseous phase primarily consisted of carbon dioxide and carbon monoxide. Consideration of external hydrogen, introduced during hydrogenation, factored into composition calculations. Properties of the produced biocrude are detailed in Table 4, highlighting a remarkable energy recovery from dry black liquor to biocrude exceeding 96%. The energy recovery is defined by Equation (1).

$$\textbf{Energy Recovery} = \frac{\textbf{Mass Yield} \cdot HHV_{\text{product}}}{HHV_{\text{feed}}}. \quad (1)$$

Table 4: Properties of produced biocrude

Carbon recovery (m-%)	93.3
Energy recovery (%)	96.1
Elemental analysis (m-%)	
C	75.8
H	9.4
O	14.8
HHV (MJ/kg)	39.4[a]
	34.9[b]

[a] Derived from Aspen plus
[b] Calculated by using modified Dulong's equation (eq 7.)

However, the higher heating value from Aspen plus data (39.4 MJ/kg) seemed inflated compared to reported literature values, prompting a recalibration using modified Dulong's equation (Hosokai et al. (2016)),

$$\text{LHV [MJ/kg]} = 38.2m_{\text{C}} + 84.9\left(m_{\text{H}} - \frac{m_{\text{O}}}{8}\right) - 0.5\,, \quad (2)$$

yielding 34.9 MJ/kg. This aligns more closely with reported literature values and underscores the significance of methodological considerations (Moser et al. 2021). Notably, the O/C ratio

decreased from 0.9 in black liquor to 0.2 in biocrude, reflecting a favourable carbon content consistent with literature (Duangkaew et al. 2022).

Examining the impact of temperature, pressure, and feed rate on yields via sensitivity analyses revealed nuanced trends. Biocrude yields exhibited a slow decline with increasing temperature until 420 °C, beyond which gas yields surged rapidly leading to decrease in biocrude yield (Figure 4). Similar phenomena have been observed in other studies (Li et al. 2019, Yang et al. 2018), emphasizing the importance of temperature in governing gasification reactions. Qian et al. 2021 built equilibrium-based simulation model for hydrothermal liquefaction of chlorella. The model predicted higher biocrude yields compared to experimental studies which is something to be considered since the model built up in this work is also based on same assumptions and property methods. However, experimental data for continuous hydrothermal liquefaction of black liquor remains limited, necessitating a reliance on batch reactor-derived data for insights.

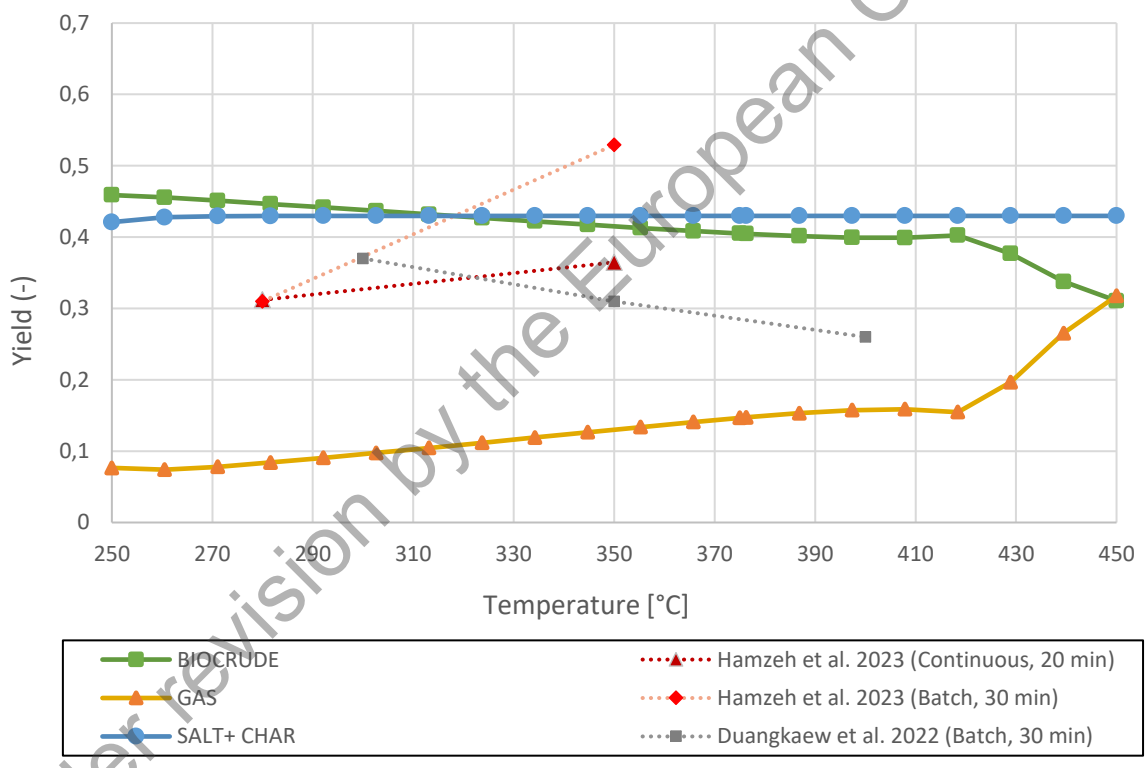

Figure 4: Mass yields per dry black liquor in 300 bar including some literature derived biocrude yield results

Pressure proved to be a determinant factor, with biocrude yields steadily increasing within the hydrothermal liquefaction zone (Figure 5). However, operational considerations, such as equipment tolerance and capital investments, impose limitations on pressure optimization.

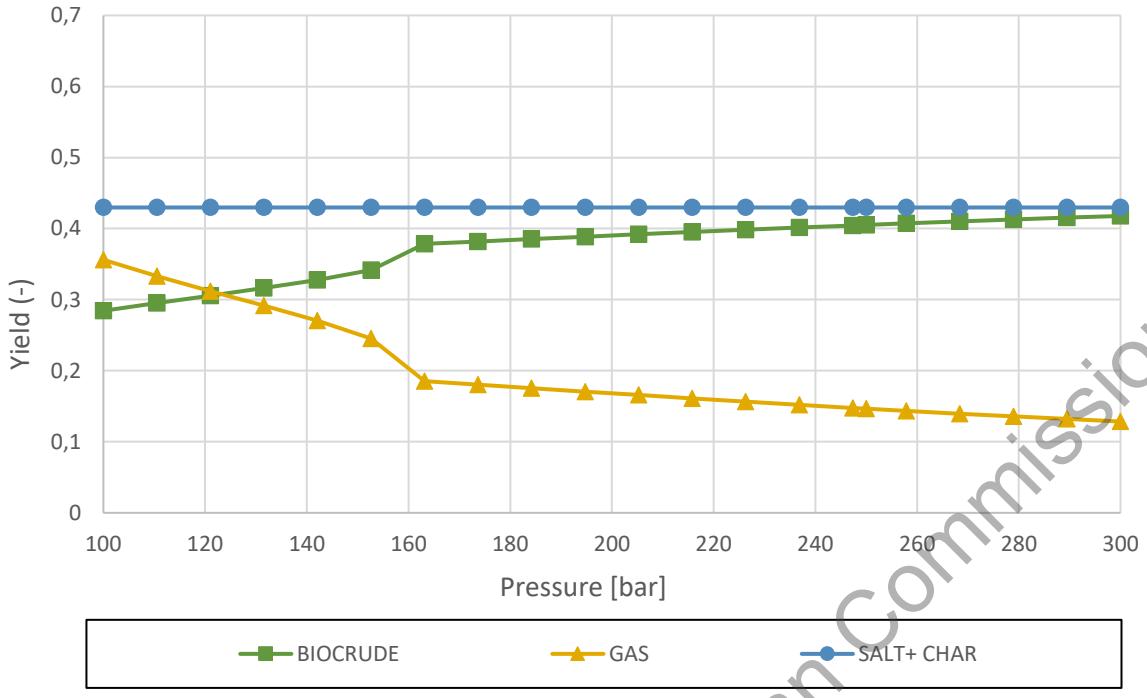

Figure 5: Mass yield per dry black liquor in 375 °C

Feed rate variations demonstrated the highest biocrude yield with pure weak black liquor (Figure 6), accompanied by a substantial increase in gas yields due to intensified hydrolysis reactions. Notably, drying weak black liquor for efficient reactor mixing and energy recovery becomes pivotal for realizing high biocrude yields.

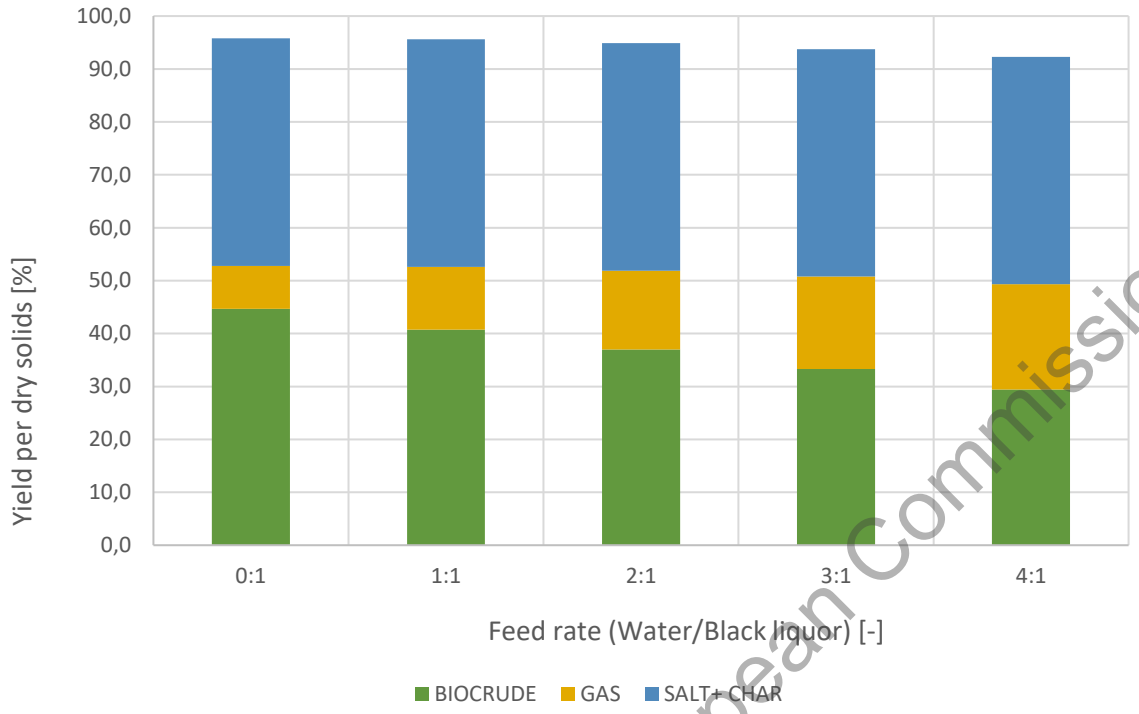

Figure 6: The effect of feed rate to yield of the products under temperature of 375 °C and pressure of 300 bar

Sensitivity analysis, assessing the influence of different model compounds on biocrude composition, revealed minor variations in results (Table 5). The discrepancy was most notable in gas formation, yet detailed examination revealed that the amount of hydrogen produced remained consistent across both cases. While the choice of model compounds impacts results, functional groups exert a more pronounced influence on product outcomes than specific compound selection.

Table 5: Sensitivity Analysis Based on Different Model Compounds of Biocrude

	Case 1	Case 2	Difference [%]
Yields [m-%]			
Biocrude	48.0	49.8	3.8
Solid (salts + char)	44.5	44.5	0.0
Gas	7.5	4.9	34.3
Carbon recovery [m-%]	93.4	96.4	3.2
Elemental analysis [m-%]			
C	75.8	75.3	0.7
H	9.4	8.8	6.7
O	0.14	0.15	7.8
Energy recovery [%]	97.2	97.8	0.6
HHV [MJ/kg]	34.9	34.0	2.4
O/C -ratio	0.20	0.21	8.5

Overall, both investigated cases exhibited relatively low variations in results. The most significant difference was observed in gas formation, where Case 1 led to higher amounts. A closer examination revealed nearly identical hydrogen production in both cases, indicating that the variation was predominantly due to carbon monoxide differences in Case 2.

In comparison with other studies, the model appears to overestimate gas production, likely attributable to the assumption of equilibrium post-reactor. The real-world limitations of continuous processes, where equilibrium is not always attainable, pose challenges. This study's departure from the simplified model compounds used by Lappalainen, chosen for a different feedstock, underscores the need for nuanced approaches in black liquor modelling.

The sensitivity analysis emphasized the robustness of the model, revealing that specific model compounds had minimal impact on results. While careful selection of model compounds is crucial, the overarching influence of functional groups on product outcomes emerged as a vital consideration. The model's tendency to overestimate gas production reinforces the necessity for more experimental data from continuous test runs.

Determining optimal process parameters for black liquor hydrothermal liquefaction is multifaceted, considering factors beyond biocrude quality and quantity. Challenges encompass the demanding nature of the process, the need for efficient recovery of cooking chemicals in pulp mill integration, and considerations for salt separation under extreme operating

conditions. Continuous hydrothermal liquefaction studies for black liquor remain sparse, underscoring the need for more accurate reaction pathways and a deeper understanding of the effect of cooking chemicals. Optimization of parameters must consider challenges such as equipment tolerances, capital investments, and the complex interplay of feedstock characteristics. More studies, especially in continuous hydrothermal liquefaction of black liquor, are imperative for realistic process modelling and cost evaluation before industrial-scale deployment.

2.3 Conclusion of the scale-up model

The Aspen Plus modelling tool could be used for the modelling, even there was not available specific reactor models for HTL. The model predicts high yield of biocrude (48 %) and low generation of gas (7.7 %) that are following the gained results in the literature and in our experiments. The quality of the biocrude is good (O_2 < 15 %), the predicted energy recovery very high (> 95 %). The model predicts are expected the gasification happening above 420 °C. Elevated pressure enhances the biocrude yield and decreases the gas production, as we have observed in our test runs. The model in addition predicts that the low dilution rate of BL is beneficial the biocrude yield (maximum at 0:1).

3 CFD modelling report

3.1 The conceptual design of the IHTL reactor

The basic idea of the IHTL reactor is two-fold; firstly, it creates a cavity to the HTL reaction having desired residence time for complete reaction, and secondly it creates a conditions to the salt separation. The separation of salts basis on the fact that salts practically have zero solubility in super-critical water (Lappalainen et al., 2020). Salts are of two types; type-1 that created in the super-critical water a high-density brine, and type-2 that form crystals. Both can be separated gravimetrically (Lappalainen et al. 2020). To enable both desired features HTL and salt separation a dual reactor design depicts in Figure 7 was designed. Third feature in the design is the utilization of Flushing waters that form a protective inert flow on the walls of the reactor, as salts, especially type-2 salts tend to be stuck on the reactor walls causing blockage.

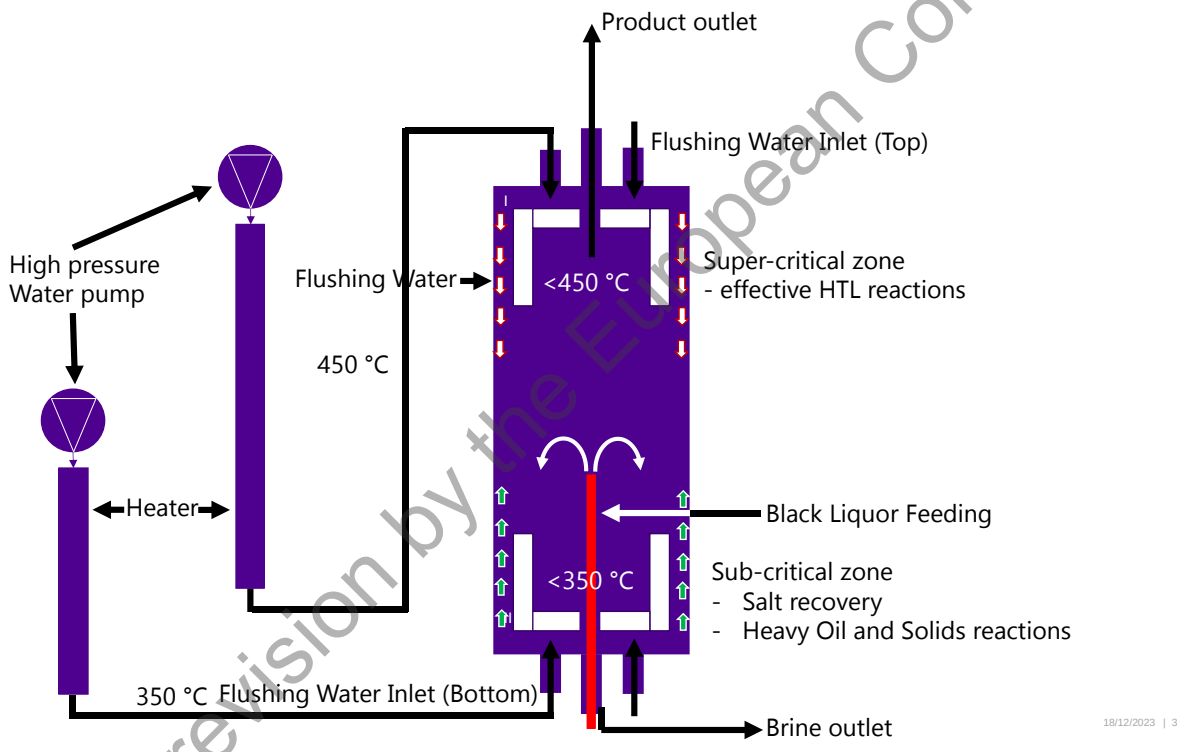

Figure 7. The novel reactor design for IHTL that combines HTL and salt separation in super-critical conditions.

The desired temperatures are in the top part of the reactor above super-critical conditions (> 220 bar, 374 °C) and below gasification temperatures (< 450 °C). The relatively high reaction temperature also provides fast reaction, and the reactor volume can be kept relatively small, as the HTL happens in just few minutes. At the bottom of the reactor that salts must be solved back to the water and thus the conditions are sub-critical below 350 °C. In the EHTA, the flushing fluids were arranged by two additional high-pressure pumps and controllable electrical heaters. The HTL-product is collected from the top of the reactor and the salty water, brine from the bottom of the reactor.

3.2 CFD modelling of the reactor

The measurement of the reactor conditions is difficult as the reactor has high pressure and temperature, in addition to this, the changing the conditions and reactor design is time-consuming and costly. Thus, Computational Fluid Dynamics (CFD) are utilized to study the reactor conditions. On the other hand, the CFD is not straightforward, as there are countless chemical reactions in the HTL, salt separation and crystallization happening. In addition, the behaviour of the super-critical water is not supported by most of the commercial CFD software programs. Thus, in BL2F a simplified scope and approach to the CFD was selected. The basic flushing setup that was applied in the EHTA pilot (Photo 1).

Photo 1. The flushing cup of the EHTA reactor

3.3 Simulation setup

The CFD model was created in the Ansys Fluent CFD software (2021 R2). The modelling approach was 2D slide of the reactor. The reactor is rotationally symmetric and by considerable accuracy the simulation of the conditions in the slide represents the general field inside the cavity of the reactor. presents the applied dimensions. The applied mesh type was Quadrilateral, having size of 0.25 mm. The total number of elements was 360 907. The Product outlet from the top of the reactor and the brine outlet were defined boundary conditions of flow rates. The inlets, two flushing fluids and the feed as velocity inlets to the specified opening.

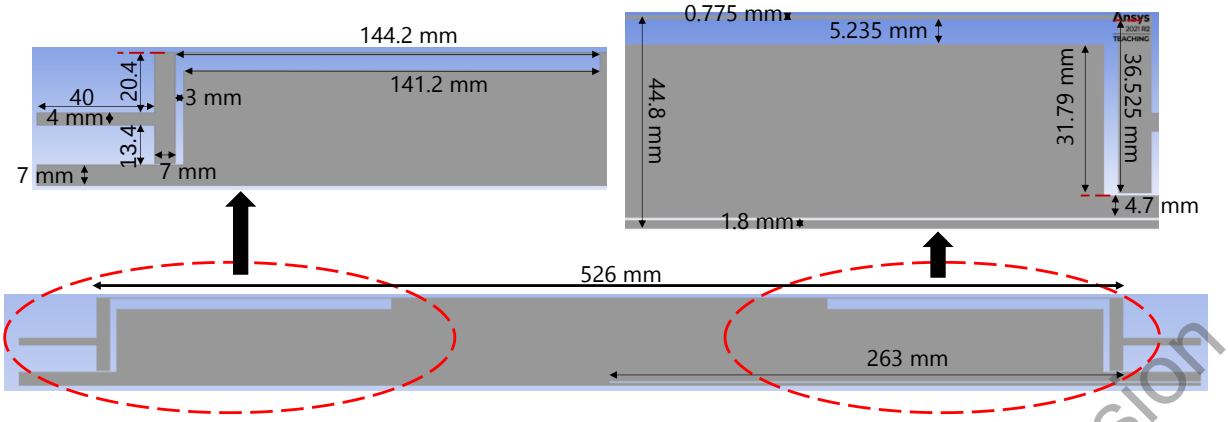

Figure 8. The applied dimensions in the CFD modelling

The simulation geometry and conditions were carefully selected to fit the test runs. The temperature was set to 400 °C and the pressure to 250 bar (Table 6).

Table 6. The reactor conditions applied in the CFD model

Property	Value
Temperature	400 °C
Pressure	250 bar
Supercritical water Density	166.58 kg/m^3
Supercritical water Viscosity	2.92e-^{05} kg/(m.s)
Specific Heat	13032 J/(Kg.K)
Thermal conductivity	0.16493 W/(m.K)
Turbulence Model	SST k-omega

The simulation conditions were varied in order to study the effectiveness of the design in order to check the Flushing potential and the mixing of the feed flow. In addition, the temperature levels were also modified in the simulations.

Table 7. The simulation conditions applied in the different simulations

	Simulation conditions	
	Velocity	Temperature
Flushing (Top)	0.4 m/s – 0.8 m/s	387.1 °C - 450 °C
Flushing (Bottom)	0.4 m/s – 0.8 m/s	350 °C – 364.6 °C
Feed	0.49 m/s– 0.99 m/s	350 °C – 360.3 °C

3.4 Simulation results

The simulations were made to study the effect of the velocities and the temperature. In the three first ones, the velocities of the feeding flows were increased to see the changes in the flow patterns and in the temperature distributions, with flow rates of small, medium, and high velocities. The fourth one had elevated temperature levels. The flow patterns and the temperature figures are presented in the Figures 9 to 16.

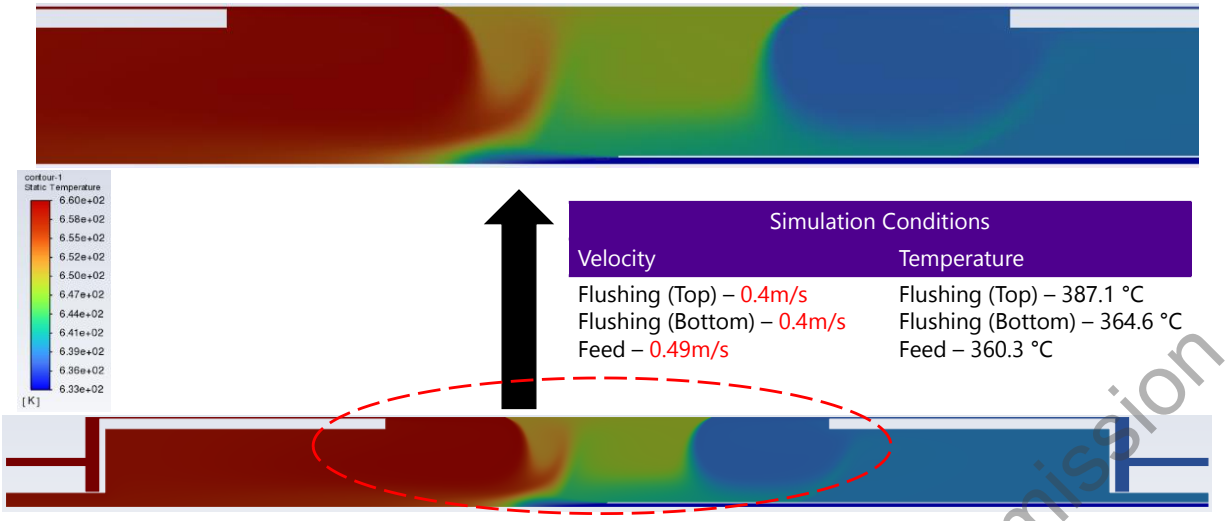

Figure 9. The velocity pattern of the simulation 1 – slow flow

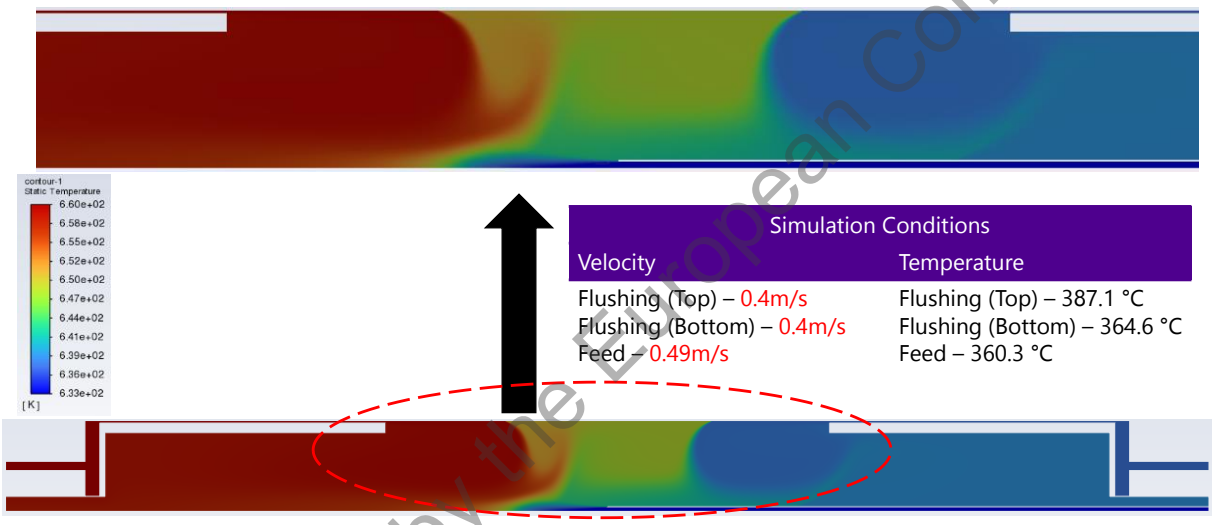

Figure 10. The temperature distribution of the simulation 1 - slow flow

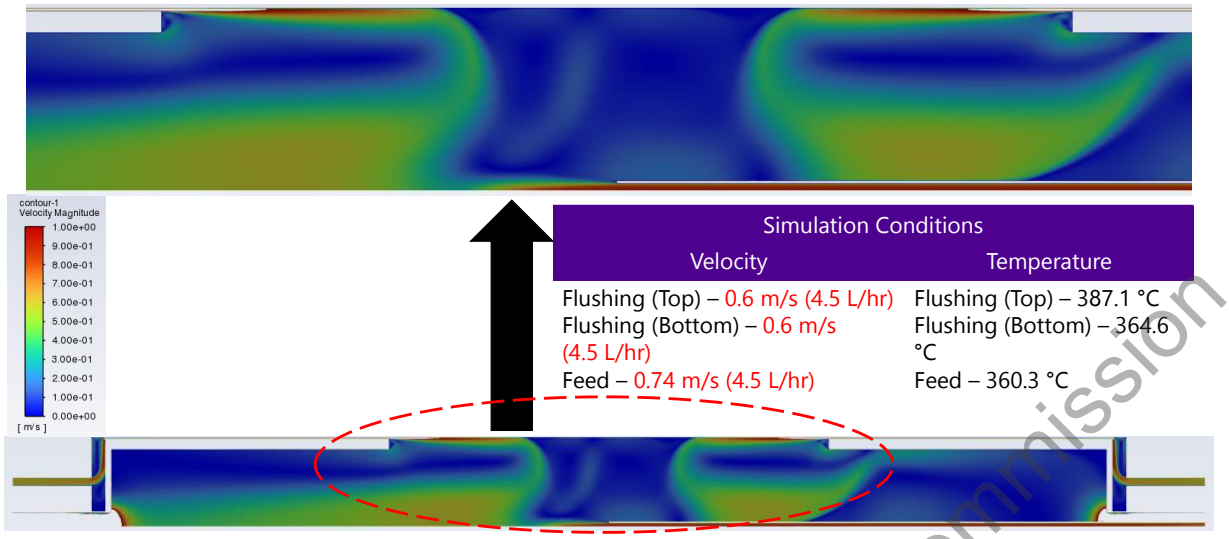

Figure 11. The velocity pattern of the simulation 2 – medium flow

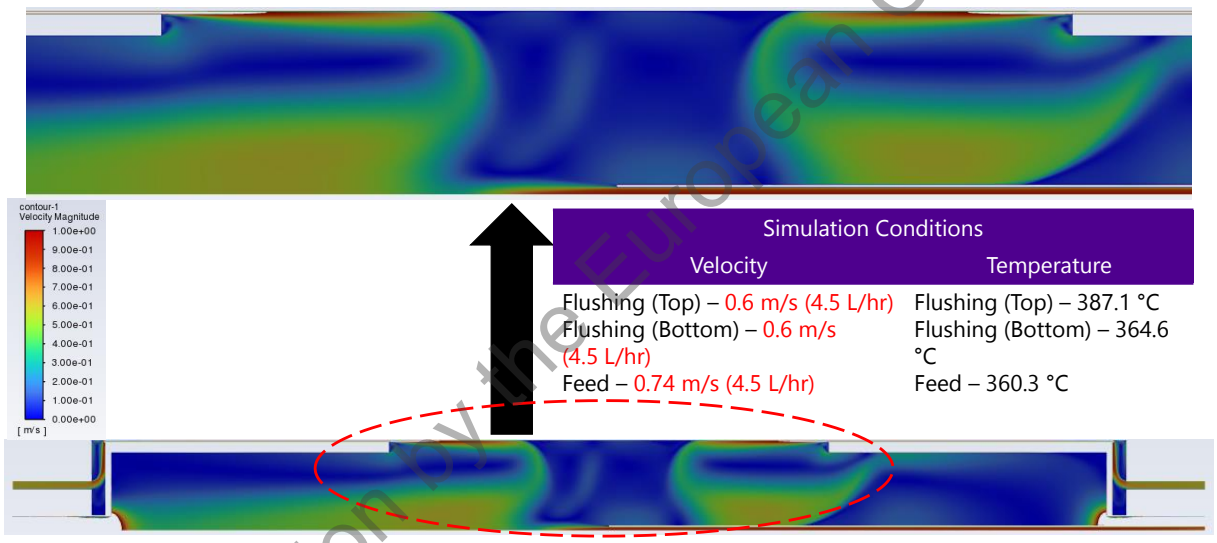

Figure 12. The temperature distribution of the simulation 2 - medium flow

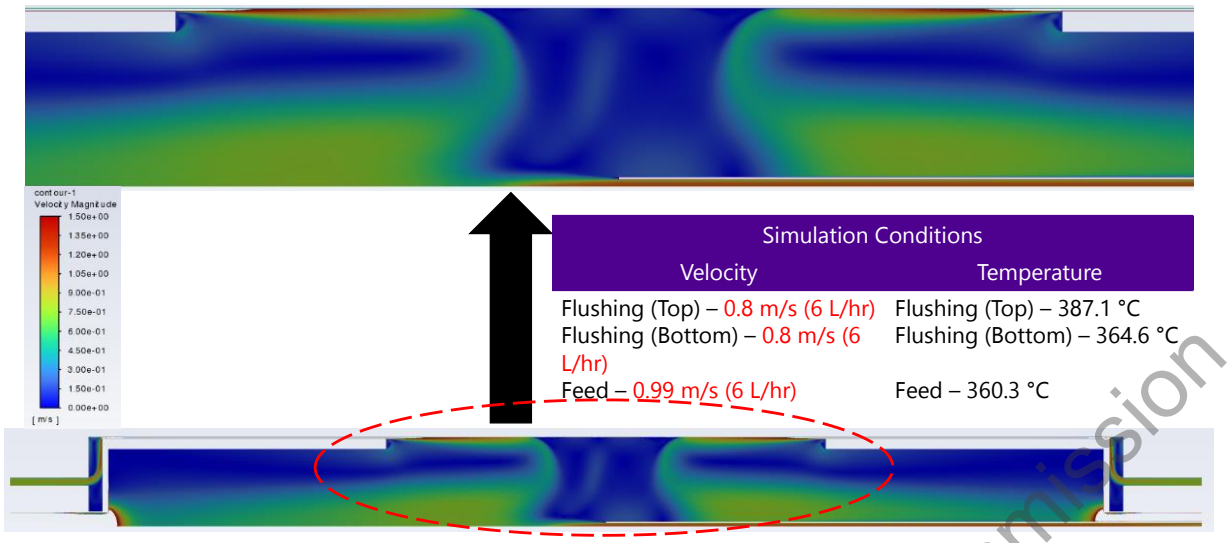

Figure 13. The velocity pattern of the simulation 3 – high flow

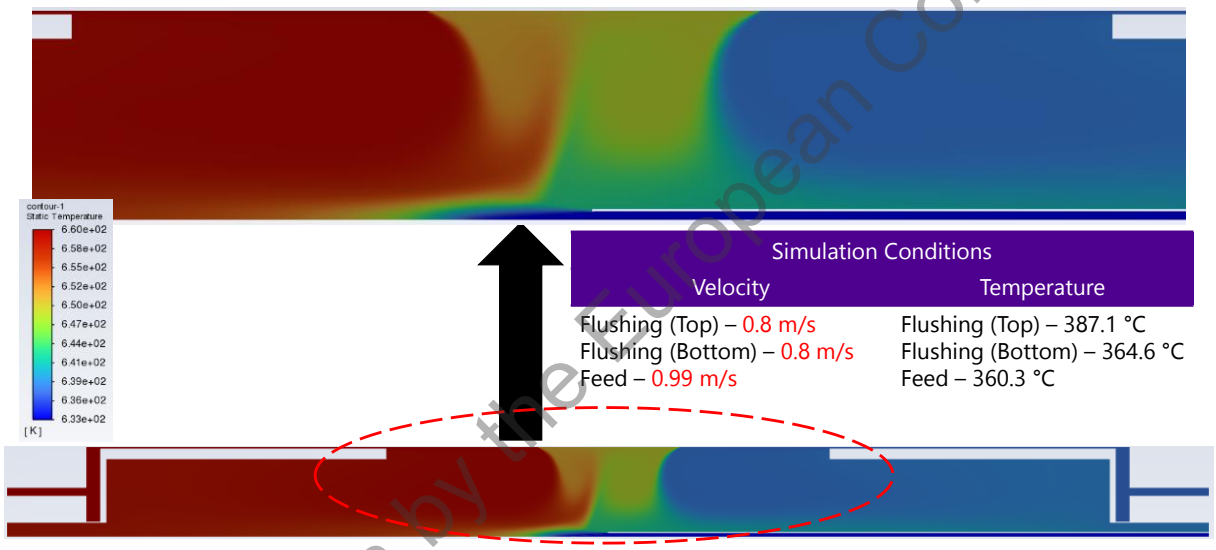

Figure 14. The temperature distribution of the simulation 3 - high flow

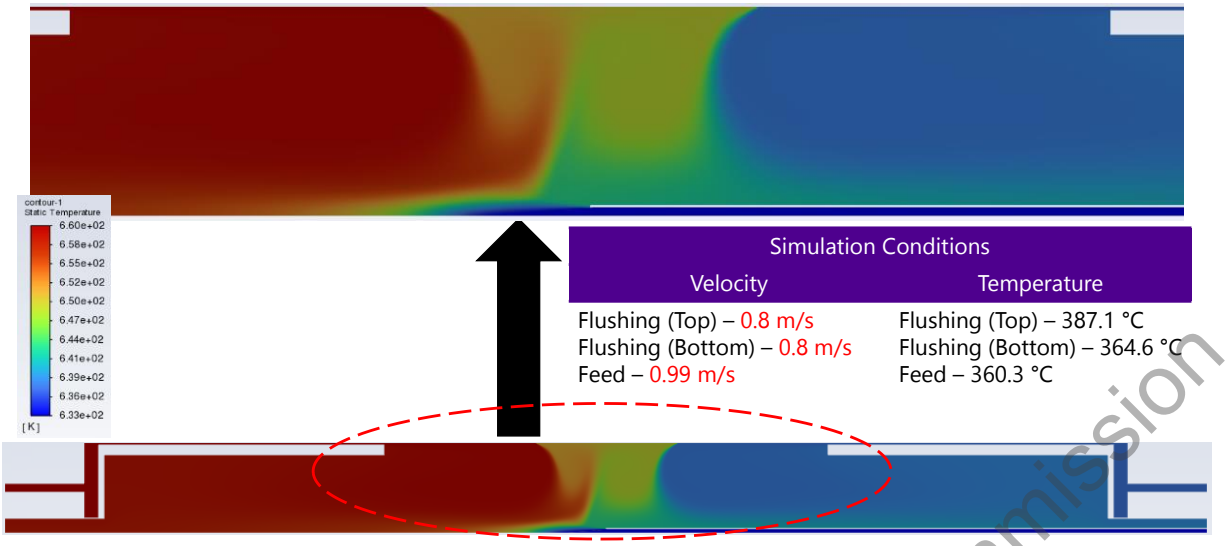

Figure 15. The velocity pattern of the simulation 4 – Elevated temperatures

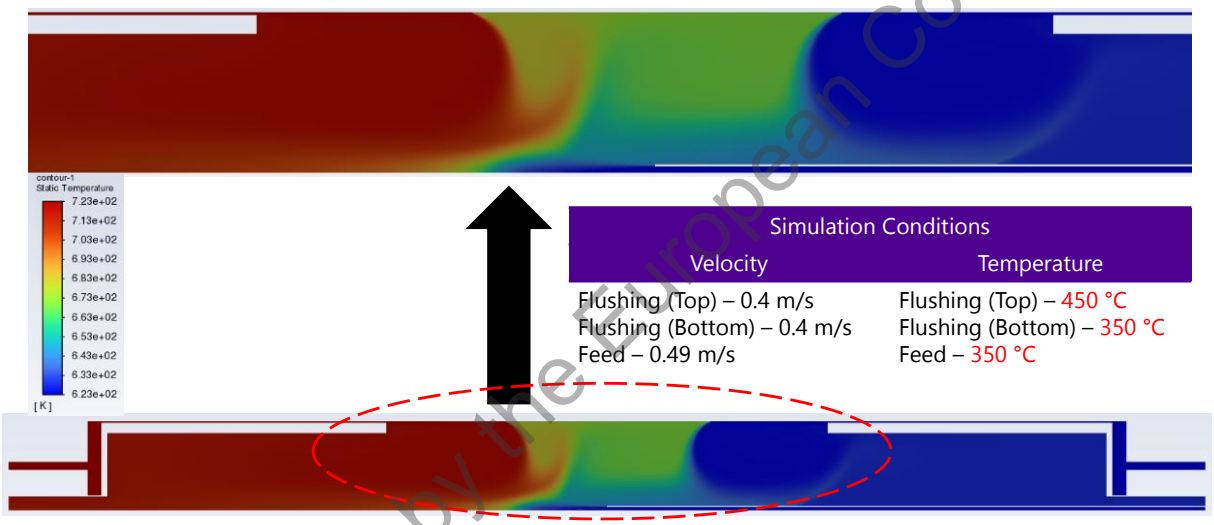

Figure 16. The temperature distribution of the simulation 4 - Elevated temperatures

3.5 Conclusion from the CFD case study

The CFD simulations show that both top and bottom flushing could be achieved. The flushing and the temperature fields were stable with the altered flow rates. Especially, the feed flow is entering the HTL zone and is well mixed with the top flushing fluid. The reaction temperature at the HTL (top) zone is homogeneous and high enough to maintaining fast reaction. The varying of the temperature does not have major effect to the flow or temperature patterns.

The test runs at least partially verify the results. The flushing seems to be working, as we have not seen any blockage or contamination at the reactor walls. In addition, the feed should be well mixed.

The CFD model can be further applied to scale up the reactor design. At the moment, we are confident that the current reactor design can be the applied as a basis for the demonstration plant design. Naturally, the accuracy of the model is questionable, but has some prediction capability.

4 Bibliography

Duangkaew, N., Pattaraprakorn, W., Grisdanurak, N., Neramittagapong, S. (2022). Utili-zation of black-liquor by hydrothermal liquefaction. Materials Today: Proceedings, 2023, Vol.75, pp. 99-105.

Hamzeh, Y., Chirat, C., Haarlemmer, G., Lachenal, D., Ashori, A., Mortha, G., Demey Cedeno, H. (2023). Extraction of phenolic compounds from hydrothermal processing of black liquor: Effect of reactor type and pH of recovered liquid phase. Chemical engineer-ing journal, 2023, Vol.470.

Hosokai, S., Matsuoka, K., Kuramoto, K., Suzuki, Y., (2016). Modification of Dulong's formula to estimate heating value of gas, liquid and solid fuels. Fuel Processing Technol-ogy, 2016, Vol.152, pp. 399-405.

Lappalainen, J. (2018). Simulation model for hydrothermal liquefaction reactions. Tampere University of Technology, p. 75.

Lappalainen, J., Baudouin, D., Hornung, U., Schuler, J., Melin, K., Bjelić, S., ... & Joronen, T. (2020). Sub-and supercritical water liquefaction of kraft lignin and black liquor derived lignin. *Energies*, *13*(13), 3309.

Li, H., Liu, Z., Wang, M., Lu, J., Bultinck, T., Wang, Y., Wang, X., Zhang, Y., Lu, H., Duan, N., Li, B., Zhang, D., Dong, T. (2019). Hydrothermal conversion of anaerobic wastewater fed microalgae: effects of reaction temperature on products distribution and biocrude properties. IET Renewable Power Generation, 2019, Vol.13, pp. 2215-2220.

Magdeldin, M., Järvinen, M. (2020). Supercritical water gasification of Kraft black liquor: Process design, analysis, pulp mill integration and economic evaluation. Applied Energy, 2020, Vol.262, p. 18.

Moser, L., Penke, C., Batteiger, V. (2021). An In-Depth Process Model for Fuel Production via Hydrothermal Liquefaction and Catalytic Hydrotreating. Processes, 2021, Vol.9, p. 1172.

Ong, B.H.Y, Walmsley, T.G., Atkins, M.J., Walmsley, M.R.W. (2018). Hydrothermal liq-uefaction of Radiata Pine with Kraft black liquor for integrated biofuel production. Journal of Cleaner Production, 2018, Vol.199, pp. 737-750.

Qian, L., Ni, J., Xu, Z., Wang, S., Gu, H., Xiang, D. (2021). Biocrude Production from Hy-drothermal Liquefaction of Chlorella: Thermodynamic Modelling and Reactor Design. Energies, 2021, Vol.14 (20), p. 9.

Woerner, M., Hornung, U., Dahmen, N. (2022). Hydrothermal Liquefaction of Black Liq-uor. EUBCE, p. 8.

Yang, J., Shin, H., Ryu, Y., Lee, C. (2018). Hydrothermal liquefaction of Chlorella vulgaris: Effect of reaction temperature and time on energy recovery and nutrient recovery. Journal of Industrial and Engineering Chemistry, 2018, Vol.68, pp. 267-273.

Appendix A. Process scale-up model flowsheet